$CsPb(I_xBr_{1-x})_3$ solar cells

Science Bulletin 64 (2019) 1532–1539

Contents lists available at ScienceDirect

Science Bulletin

journal homepage: www.elsevier.com/locate/scib

Science Bulletin
www.scibull.com

Progress

$CsPb(I_xBr_{1-x})_3$ solar cells ☆

Xue Jia [a,b], Chuantian Zuo [c], Shuxia Tao [d], Kuan Sun [e], Yixin Zhao [f], Shangfeng Yang [g], Ming Cheng [h], Mingkui Wang [i], Yongbo Yuan [j], Junliang Yang [j], Feng Gao [k], Guichuan Xing [l], Zhanhua Wei [m], Lijun Zhang [n], Hin-Lap Yip [o], Mingzhen Liu [p], Qing Shen [q], Longwei Yin [r], Liyuan Han [s], Shengzhong Liu [t], Lianzhou Wang [u], Jingshan Luo [v,*], Hairen Tan [w,*], Zhiwen Jin [x,*], Liming Ding [a,b,*]

[a] Center for Excellence in Nanoscience (CAS), Key Laboratory of Nanosystem and Hierarchical Fabrication (CAS), National Center for Nanoscience and Technology, Beijing 100190, China
[b] University of Chinese Academy of Sciences, Beijing 100049, China
[c] CSIRO Manufacturing, Bag 10, Clayton South, Victoria 3169, Australia
[d] Center for Computational Energy Research, Department of Applied Physics, Eindhoven University of Technology, 5600MB Eindhoven, The Netherlands
[e] MOE Key Laboratory of Low-grade Energy Utilization Technologies and Systems, Chongqing University, Chongqing 400044, China
[f] School of Environmental Science and Engineering, Shanghai Jiao Tong University, Shanghai 200240, China
[g] Department of Materials Science and Engineering, University of Science and Technology of China, Hefei 230026, China
[h] Institute for Energy Research, Jiangsu University, Zhenjiang 212013, China
[i] Wuhan National Laboratory for Optoelectronics, Huazhong University of Science and Technology, Wuhan 430074, China
[j] School of Physics and Electronics, Central South University, Changsha 410083, China
[k] Department of Physics, Chemistry and Biology, Linköping University, SE-58183 Linköping, Sweden
[l] Institute of Applied Physics and Materials Engineering, University of Macau, Macau 999078, China
[m] College of Materials Science & Engineering, Huaqiao University, Xiamen 361021, China
[n] College of Materials Science and Engineering, Jilin University, Changchun 130012, China
[o] State Key Laboratory of Luminescent Materials and Devices, South China University of Technology, Guangzhou 510640, China
[p] Center for Applied Chemistry, School of Materials and Energy, University of Electronic Science and Technology of China, Chengdu 611731, China
[q] Faculty of Informatics and Engineering, The University of Electro-Communications, Tokyo 182-8585, Japan
[r] School of Materials Science and Engineering, Shandong University, Jinan 250061, China
[s] State Key Laboratory of Metal Matrix Composites, School of Materials Science and Engineering, Shanghai Jiao Tong University, Shanghai 200240, China
[t] Shaanxi Key Laboratory for Advanced Energy Devices, Shaanxi Normal University, Xi'an 710119, China
[u] Nanomaterials Centre, School of Chemical Engineering, The University of Queensland, St Lucia, QLD 4072, Australia
[v] Institute of Photoelectronic Thin Film Devices and Technology, Nankai University, Tianjin 300350, China
[w] College of Engineering and Applied Sciences, Nanjing University, Nanjing 210093, China
[x] School of Physical Science and Technology, Lanzhou University, Lanzhou 730000, China

ARTICLE INFO

Article history:
Received 6 August 2019
Received in revised form 9 August 2019
Accepted 10 August 2019
Available online 16 August 2019

Keywords:
Perovskite solar cells
Cesium lead halide perovskites
Power conversion efficiency
Stability

ABSTRACT

Owing to its nice performance, low cost, and simple solution-processing, organic-inorganic hybrid perovskite solar cell (PSC) becomes a promising candidate for next-generation high-efficiency solar cells. The power conversion efficiency (PCE) has boosted from 3.8% to 25.2% over the past ten years. Despite the rapid progress in PCE, the device stability is a key issue that impedes the commercialization of PSCs. Recently, all-inorganic cesium lead halide perovskites have attracted much attention due to their better stability compared with their organic-inorganic counterpart. In this progress report, we summarize the properties of $CsPb(I_xBr_{1-x})_3$ and their applications in solar cells. The current challenges and corresponding solutions are discussed. Finally, we share our perspectives on $CsPb(I_xBr_{1-x})_3$ solar cells and outline possible directions to further improve the device performance.

1. Introduction

Organic-inorganic hybrid perovskite solar cells (PSCs) have attracted great attention because of their excellent optoelectronic properties, such as high absorption coefficients [1], tunable optical bandgaps [2], high carrier mobility [3], long charge-carrier diffusion length [4], and low exciton binding energy [5]. The power conversion efficiency (PCE) of organic-inorganic hybrid PSCs has

☆ Dedicated to the 70th Anniversary of the Founding of New China.

* Corresponding authors.
E-mail addresses: jingshan.luo@nankai.edu.cn (J. Luo), hairentan@nju.edu.cn (H. Tan), jinzw@lzu.edu.cn (Z. Jin), ding@nanoctr.cn (L. Ding).

https://doi.org/10.1016/j.scib.2019.08.017
2095-9273/

reached 25.2% (NREL Best Research-Cell Efficiency Chart, https://www.nrel.gov/pv/cell-efficiency.html, Accessed August 2019), starting from 3.8% in 2009 [6]. Despite much great effort has been made in photovoltaic (PV) performance [7–11], organic–inorganic hybrid PSCs still suffer from poor long-term stability, which is due to the intrinsic volatility and thermal instability of the organic components [12]. By replacing the organic cation with cesium (Cs), all-inorganic cesium lead halide perovskites may lead to stable high-efficiency devices. Owing to their excellent stability and optoelectronic properties, all-inorganic $CsPb(I_xBr_{1-x})_3$ solar cell is a hotspot in the field of perovskite solar cells and exhibit a dramatic increase in PCE (from 2.9% [13] in 2015 to 17.06% [14] in 2018) in the last few years (Fig. 1).

In this progress report, we first discuss the properties of $CsPbX_3$, including crystal structure, stability, and dielectric properties. Then, we systematically review the recent progress on $CsPb(I_xBr_{1-x})_3$ solar cells in four aspects: phase stability, crystallization control, low-temperature preparation, and defect passivation. Finally, we propose some important issues and future research directions for developing stable high-efficiency $CsPb(I_xBr_{1-x})_3$ solar cells.

2. Properties of $CsPbX_3$

Although $CsPbX_3$ (X is halogen) perovskites were first reported in 1893 [15], their crystal structure and photoconductivity were not investigated until 1958 [16]. $CsPbI_3$ solar cells were first reported in 2015, giving a PCE of 2.9% [13]. $CsPbX_3$ has four crystal structures [17]: cubic phase (α), tetragonal phase (β), orthorhombic phase (γ), and non-perovskite phase (δ) (Fig. 2a). For $CsPbI_3$, the black cubic perovskite phase (α-$CsPbI_3$) has a direct bandgap (E_g) of 1.73 eV, which is suitable for PV applications and especially desirable for tandem solar cells with crystalline silicon [20]. Unfortunately, α-$CsPbI_3$ is only thermodynamically stable at temperatures above 300 °C, and easily transforms to an undesirable non-perovskite δ-phase (E_g = 2.82 eV) under ambient conditions. The highly symmetric α-$CsPbI_3$ can distort to a tetragonal phase, followed by a further change to orthorhombic phase, when the temperature decreases [17]. Considering the formation energies of the four crystals, orthorhombic phase is the most stable one among the perovskite polymorphs, and it is less stable than the non-perovskite δ-phase (Fig. 2b) [18]. The bandgap of the non-perovskite phase is too wide for obtaining good photovoltaic performance. Thus, one of the key challenges in making highly efficient all-inorganic $CsPb(I_xBr_{1-x})_3$ solar cells is to improve their phase stability under ambient conditions.

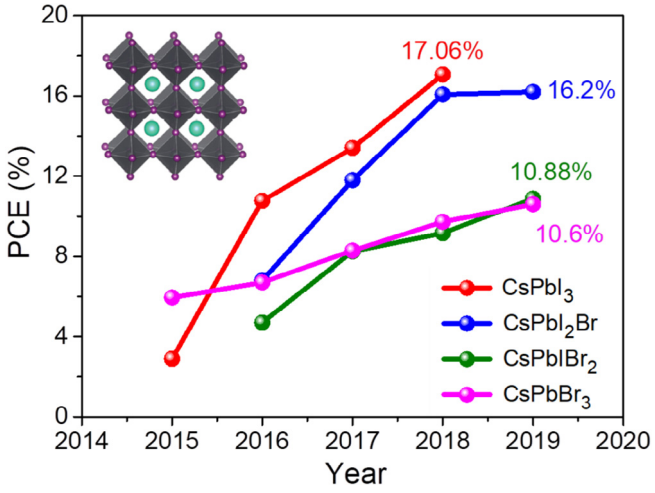

Fig. 1. Progress for $CsPbI_3$, $CsPbI_2Br$, $CsPbIBr_2$, and $CsPbBr_3$ solar cells.

The phase transition, the exciton binding energy (R^*), the effective mass (μ), and the effective dielectric constant (ε_{eff}) are important factors determining the photovoltaic performance of all-inorganic perovskites. These factors were systematically studied by Yang et al. in 2017 [19]. Temperature-dependent transmission spectra of $CsPbX_3$ were measured in a wide temperature range (4.2 – 270 K) (Fig. 2c). The bandgaps of $CsPbX_3$ increased with temperature monotonically (4.2 – 270 K). This indicates that all-inorganic perovskites do not make phase transitions in this temperature range, which is quite different from that for organic–inorganic hybrid perovskites. In addition, the bandgap increases from $CsPbI_3$ to $CsPbI_2Br$ and $CsPbBr_3$, suggesting that the halogen in $CsPbX_3$ crystal can tune their bandgaps. R^* and μ were obtained from low-temperature magneto-transmission spectroscopy [19], and they both increased with bandgap (Fig. 2d). ε_{eff} for $CsPbX_3$ was calculated from R^* and μ. Compared with the corresponding values of organic-inorganic hybrid counterparts, ε_{eff} did not change very much for a given lead halide cage, but decreased with decreasing halogen mass.

3. Progress of $CsPb(I_xBr_{1-x})_3$ solar cells

3.1. Phase stability

A key issue for $CsPb(I_xBr_{1-x})_3$ solar cells is the phase stability of α-$CsPbI_3$, since the black phase (α-$CsPbI_3$) can easily transform to non-perovskite yellow phase (δ-$CsPbI_3$) at room temperature. To solve this problem, several approaches were used, such as reducing the crystal size or dimensionality, adding additives, and doping element.

When the crystal size or dimensionality is reduced, $CsPbI_3$ tends to convert to a more symmetric crystal structure (cubic phase). Swarnkar et al. [21] developed stable α-$CsPbI_3$ quantum dots (QDs) and demonstrated that the cubic phase could be maintained for months under ambient conditions. The solar cells based on α-$CsPbI_3$ QDs gave a PCE of 10.77% with an open-circuit voltage (V_{oc}) of 1.23 V (Fig. 3a). Later, Liu et al. [26] made high-quality $CsPbI_3$ QDs by using PbI_2/GeI_2 mixture, which showed improved chemical stability and ~100% photoluminescence quantum yield (PL QY). The solar cells based on $CsPbI_3$ QDs gave a PCE of 12.15%, and could maintain 85% of its original PCE after being stored in dry air for more than 90 days. However, the fabrication process for QDs cells is complex, thus it is difficult to make scalable production. By incorporating a small amount of large cation into $CsPb(I_xBr_{1-x})_3$ to form quasi-2D perovskites or mixed 2D/3D perovskites, α-$CsPbI_3$ phase can be stabilized. Large cations such as butyl ammonium (BA) [27], phenylethylammonium (PEA) [28,29], diethylenetriamine (DETA) [30], and ethylenediamine (EDA) [31] were used. Jiang et al. [22] successfully obtained quasi-2D perovskites $PEA_2Cs_{n-1}Pb_nI_{3n+1}$ by introducing phenylethylammonium iodide (PEAI) into $CsPbI_3$ (Fig. 3b). The solar cells delivered a PCE of 12.4% and the phase transition was significantly suppressed.

Adding additive is another effective method to stabilize α-$CsPbI_3$ phase, since the additive could tailor the surface energy, reduce the grain size, and passivate surfaces. Wang et al. [23] added a small amount of sulfobetaine zwitterion into $CsPbI_3$ precursor solution and obtained $CsPbI_3$ films with grain size of ~30 nm. The stability of α-$CsPbI_3$ phase was improved. Because of the steric effect of the zwitterion long ligands, and the electrostatic interaction between zwitterion and PbI_2·DMSO colloids, the zwitterions can suppress $CsPbI_3$ crystallization, thus reducing the grain size (Fig. 3c). The resulting solar cells gave a PCE of 11.4%. Polymers can be effective additives. Recently, Li et al. [24] demonstrated that polyvinylpyrrolidone (PVP) played an important role in stabilizing α-$CsPbI_3$ phase (Fig. 3d). The $CsPbI_3$ films showed

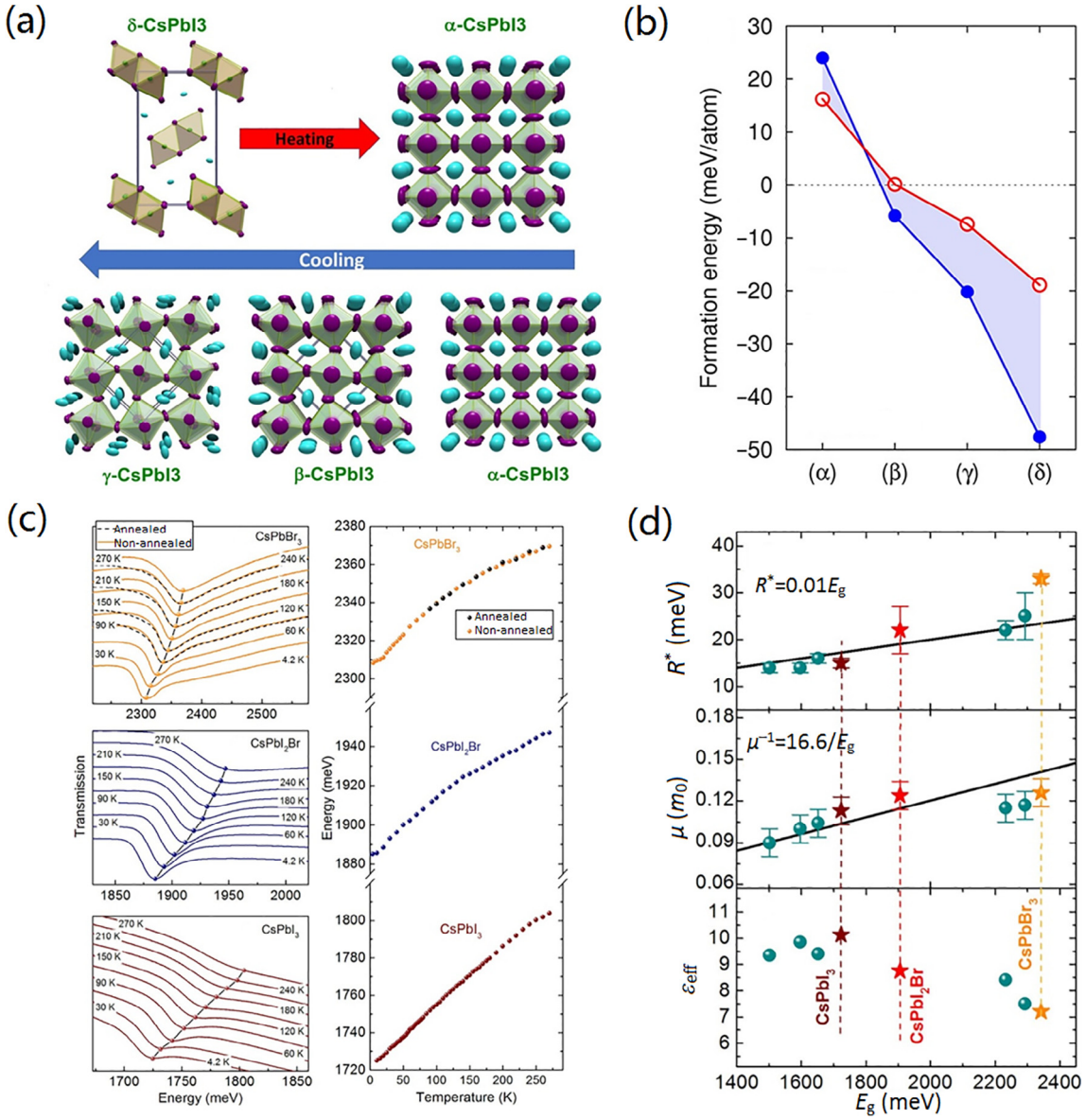

Fig. 2. (a) Phase transitions of $CsPbI_3$. Reproduced with permission [17], Copyright 2018, American Chemical Society. (b) Theoretical formation energies for 4 type crystals of $CsPbI_3$, the red circles correspond to density functional theory (DFT)/Perdew-Burke-Ernzerh (PBE) calculations, while the blue dots correspond to DFT/local density approximation (LDA) calculations. Reproduced with permission [18], Copyright 2018, American Chemical Society. (c) Temperature-dependent transmission spectra and energy of the 1s transition as a function of temperature for $CsPbBr_3$, $CsPbI_2Br$, and $CsPbI_3$. (d) R^*, μ, and ε_{eff} for $CsPb(I_xBr_{1-x})_3$; brown, red, and yellow stars indicate the parameters for $CsPbI_3$, $CsPbI_2Br$, and $CsPbBr_3$, respectively. (c) and (d), reproduced with permission [19], Copyright 2017, American Chemical Society.

long carrier lifetime (338.7 ns) and long diffusion length (>1.5 μm), and the solar cells gave a PCE of 10.74%.

The low structural stability of $CsPbI_3$ is mainly due to its low Goldschmidt's tolerance factor t (~0.81), which results from the small size of Cs^+. Partially substituting B-site cation (Pb^{2+}) with smaller ions or X-site anion (I^-) with smaller halogen ions (Br^-, Cl^-) can increase t and stabilize $CsPbI_3$. The partial substitution of Pb^{2+} with different metal ions could stabilize α-$CsPbI_3$ at room temperature by increasing t and improve thermal stability of $CsPbBr_3$ (Fig. 3e) [25]. Recently, various metal ions, such as Bi^{3+} [32], Sr^{2+} [33], Mn^{2+} [34,35], Ge^{2+} [36], Ca^{2+} [37], and Eu^{2+} [38], were used for improving phase stability.

3.2. Crystallization control

Another challenge for $CsPb(I_xBr_{1-x})_3$ solar cells is to control the crystallization process to obtain high-quality perovskite films. The energy barrier for inserting Cs^+ into PbX_2 frameworks is low. CsI can react with PbX_2 quickly, thus leading to many pinholes in the films and small grain size. Dimethyl sulfoxide (DMSO) has a high boiling point (189 °C) and a strong coordination capability, when it is introduced into *N*,*N*-dimethylformamide (DMF) as co-solvent, the crystallization could be somehow suppressed. The residual DMSO could improve the film quality. Zhang et al. [39] used mixed solvent (DMF + DMSO), then used hot air flow to improve the crystallization. The $CsPbI_2Br$ solar cells gave a PCE of 12.52% and a high V_{oc} of 1.32 V. Wang et al. [40] developed a simple solvent-controlled growth (SCG) method to prepare high-quality α-$CsPbI_3$ films (Fig. 4a). The annealed $CsPbI_3$ film showed smooth surface with large grain size (>5 μm). The resulting solar cells gave a PCE of 15.7% and a certified PCE of 14.67%.

Anti-solvent (ATS) treatment could also help to control the crystal growth. Recently, Chen et al. [41] used a synergetic process consisting of gradient thermal annealing (GTA) and ATS treatment to

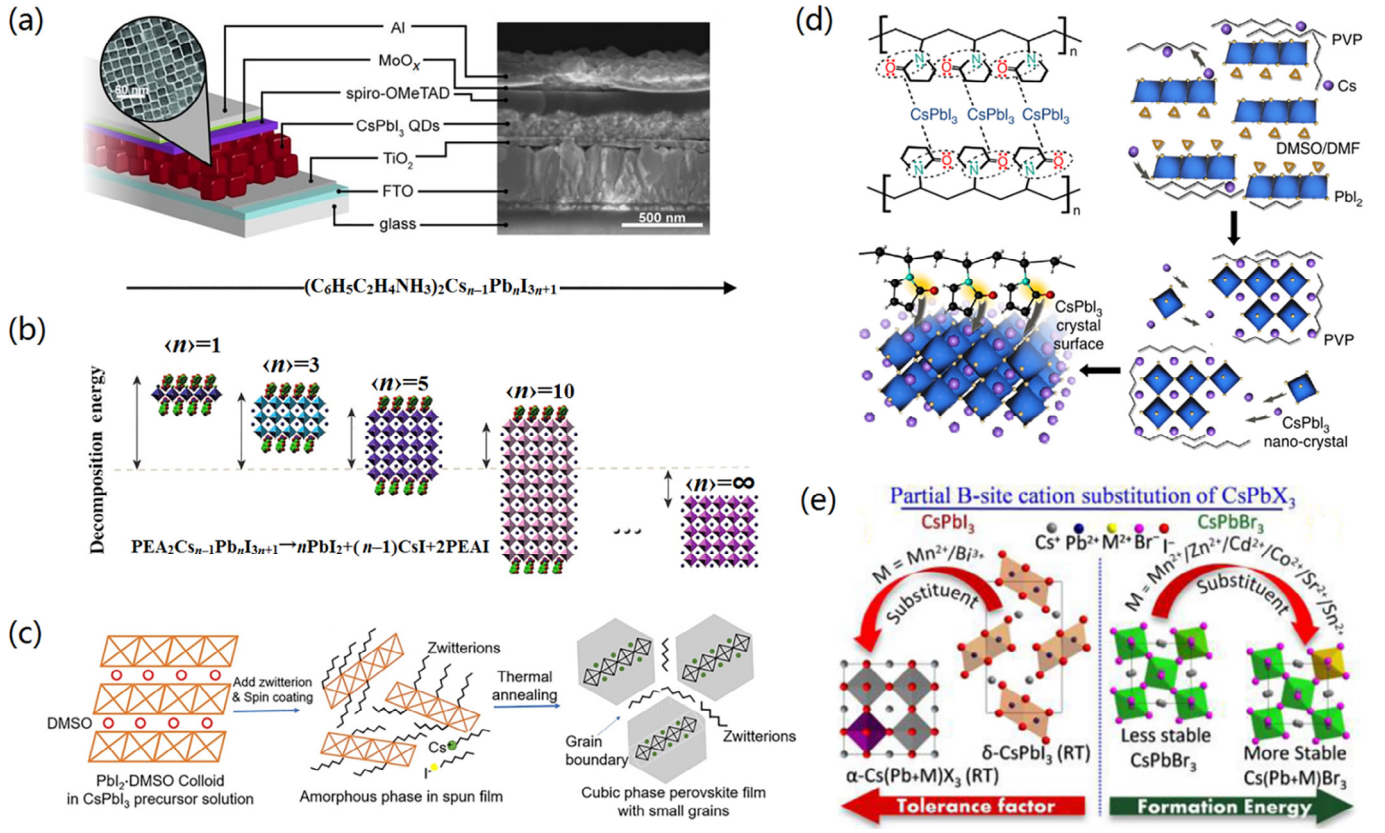

Fig. 3. (a) Schematic diagram and SEM cross-section image for $CsPbI_3$ solar cells. Reproduced with permission [21], Copyright 2016, American Association for the Advancement of Science. (b) Structures of $PEA_2Cs_{n-1}Pb_nX_{3n+1}$ and their decomposition energy from first-principles DFT. Reproduced with permission [22], Copyright 2018, Elsevier. (c) Stabilizing α-$CsPbI_3$ phase by zwitterion. Reproduced with permission [23], Copyright 2017, Elsevier. (d) Stabilizing α-$CsPbI_3$ phase by PVP. Reproduced with permission [24], Copyright 2018, Nature Publishing Group. (e) Partial substitution of Pb^{2+} by various metal ions in $CsPbX_3$. Reproduced with permission [25], Copyright 2018, American Chemical Society.

control the crystal growth, leading to a high-quality α-$CsPbI_2Br$ film with grain size of ~1 μm and a smooth surface (Fig. 4b). The GTA process slowed down the evaporation rate of the residual DMSO, thus reducing the nucleation and growth rate, and ATS method could improve the film uniformity. The resulting α-$CsPbI_2Br$ solar cells delivered a PCE of 16.07% and a stabilized PCE of 15.75%. Other strategies for controlling crystallization to improve film quality were reported, such as all-vacuum co-deposition technique [43], and hot spinning of the precursor solution [44]. Though much efforts have been made to control crystallization, further work is needed to obtain high-quality $CsPb(I_xBr_{1-x})_3$ films with large grain size and low trap density.

3.3. Low-temperature preparation

The third challenge is to make high-quality $CsPb(I_xBr_{1-x})_3$ films via a low-temperature process. In general, $CsPb(I_xBr_{1-x})_3$ films are prepared at high temperatures (>250 °C) to get a black perovskite phase, while that is energy-consuming and would limit their applications in flexible and tandem solar cells. Eperon et al. [13] successfully made black α-$CsPbI_3$ film at 100 °C by adding a small amount of HI into precursor solution (Fig. 4c). HI could decrease the phase transition temperature. Recently, Wang et al. [45] developed a facile method to make $CsPbI_2Br$ films at 100–130 °C. They prepared a new precursor by using the reaction between PbI_2 and HI in DMF. And then compact and pinhole-free films were obtained. Reducing crystallization energy barrier favors to form α-$CsPbI_2Br$ phase. The solar cells gave a PCE of 10.56%. Later, Rao et al. [42] prepared uniform and pinhole-free $CsPbI_2Br$ films by using a room-temperature solvent annealing (RTSA) method (Fig. 4d). With further post-annealing at 120 °C, the $CsPbI_2Br$ solar cells gave a PCE of 10.4%. Besides, they first made flexible $CsPbI_2Br$ solar cells, giving a PCE of 7.3%. More recently, Jiang et al. [46] obtained high-quality $CsPbI_2Br$ film at 120 °C with PbI_2(DMSO) and $PbBr_2$(DMSO) as precursors. These DMSO adducts could not only slow down the crystal growth, but also reduce the formation energy of $CsPbI_2Br$. The solar cells delivered a PCE of 13.54%, and the flexible $CsPbI_2Br$ solar cells gave a PCE of 11.73%. Zai et al. [47] made high-quality $CsPbI_2Br$ films at 100 °C by adjusting DMSO/DMF ratio in the precursor solution and the solar cells offered a PCE of 14.3%. Interestingly, partially substituting Pb with Sr could also help to make high-quality $CsPbI_2Br$ films at low temperature (100 °C) [33]. The above results demonstrate that high-quality $CsPb(I_xBr_{1-x})_3$ films could be prepared at low temperature, making all-inorganic $CsPb(I_xBr_{1-x})_3$ perovskites promising for flexible device applications.

3.4. Defect passivation

The fourth challenge is to passivate the defects to improve the performance and stability of $CsPb(I_xBr_{1-x})_3$ solar cells. The defects at the grain boundaries (GBs) and perovskite film surface could become deep traps, which act as the charge recombination centers. The defects not only cause non-radiative energy loss, leading to V_{oc} reduction, but also form the channels for the permeation of oxygen and moisture, harming device stability. Therefore, defect passivation is very important for enhancing device performance.

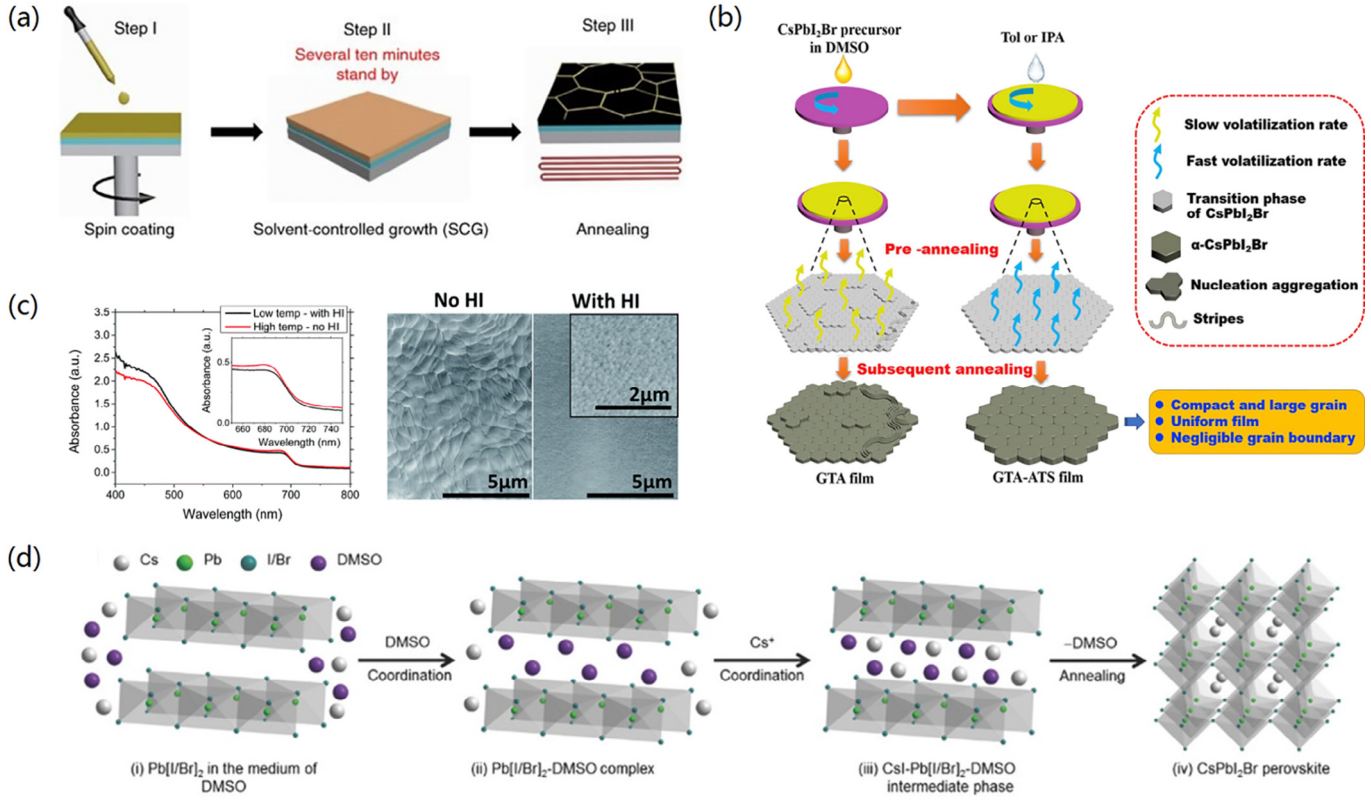

Fig. 4. (a) Preparation of $CsPbI_3$ films via SCG method. Reproduced with permission [40], Copyright 2018, Nature Publishing Group. (b) Preparation of $CsPbI_2Br$ films via GTA or GTA-ATS. Reproduced with permission [41], Copyright 2019, Elsevier. (c) Absorption spectra and SEM images of the films prepared on FTO/compact TiO_2 substrate at low and high temperatures (with and without HI). Reproduced with permission [13], Copyright 2015, Royal Society of Chemistry. (d) Preparation of $CsPbI_2Br$ films at room temperature by using RTSA method. Reproduced with permission [42], Copyright 2018, Wiley-VCH.

B-site ionic dopants (Mn^{2+} and Zn^{2+} etc.) could passivate the charge traps, improving device performance. Bai et al. [34] demonstrated that Mn^{2+} doping to $CsPbI_2Br$ could passivate the surface and GB defects, enhancing hole extraction efficiency. The best cells gave a PCE of 13.47% and a V_{oc} of 1.17 V. Recently, Sun et al. [48] found that Zn^{2+} had similar passivation function, and the GB defects were passivated by forming Cs-Zn-I/Br compound. Furthermore, Zn^{2+} could slow down the crystallization, leading to larger grain size (Fig. 5a). $CsPb_{0.9}Zn_{0.1}I_2Br$ solar cells gave a PCE of 13.6%. Zeng et al. [49] successfully made efficient and stable $CsPbI_2Br$ solar cells by adding lead acetate $Pb(Ac)_2$ into $CsPbI_2Br$ precursor solution. $Pb(Ac)_2$ distributed at the GBs, and in situ decomposed and produced PbO under high-temperature annealing (Fig. 5b). PbO at the GBs could effectively passivate the traps, reduce non-radiative recombination, favoring charge transport in $CsPbI_2Br$ films. The PCE was increased from 8.5% to 12%.

Surface post-treatment on as-cast perovskite films is another effective method for defect passivation. The surface defects can be passivated by depositing a thin poly(3-hexylthiophene) (P3HT) film on top of $CsPbI_2Br$ layer [50]. According to density functional theory (DFT) calculation, sulfur (S) atoms can passivate non-coordinated Cs^+ via bonding with Cs. S atoms can also bond with Pb, passivating the defects. A PCE of 12.02% was obtained, with a V_{oc} of ~1.32 V and an E_{loss} of ~0.5 eV. Wang et al. [14] used phenyltrimethylammonium bromide (PTABr) for the post-treatment on $CsPbI_3$ films. PTABr could passivate surface defects and make gradient Br doping into $CsPbI_3$ films (Fig. 5c). The solar cells delivered an impressive PCE of 17.06%, the record to date for $CsPb(I_xBr_{1-x})_3$ solar cells. PEAI was also used for surface defect passivation [51].

4. Conclusions and perspectives

Owing to their excellent optoelectronic properties and thermal stability, $CsPb(I_xBr_{1-x})_3$ solar cells are regarded as a promising alternative for organic-inorganic hybrid PSCs. Although much progress have been made since 2015 [13,14,52–54], the performance of $CsPb(I_xBr_{1-x})_3$ solar cells is still lower than that of organic-inorganic hybrid counterparts. It is predicted that the PCEs of $CsPbI_3$, $CsPbI_2Br$, and $CsPbIBr_2$ solar cells can reach 21.7%, 19.0%, and 16.6%, respectively [55]. The reported PCEs are still much lower than the theoretical values. Some crucial issues have to be addressed to further improve the device performance. The issues are as follows (see Fig. 6):

(1) Phase stability. Although $CsPb(I_xBr_{1-x})_3$ perovskites present good thermal stability, they still suffer from a low phase stability especially under ambient conditions. To obtain efficient and stable $CsPb(I_xBr_{1-x})_3$ solar cells, this issue should be first resolved.
(2) Crystallization control. It is very difficult to control $CsPb(I_xBr_{1-x})_3$ crystal growth and film quality, which affect device performance greatly. Additives engineering, solvents engineering, and processing conditions should be extensively explored to realize it.
(3) Interface engineering. Choosing suitable hole transport layer (HTL), electron transport layer (ETL) and interfacial layer is crucial for facilitating charge transport and reducing energy loss. Optimal choice can help to get high V_{oc}, high fill factor (FF), and high PCE.

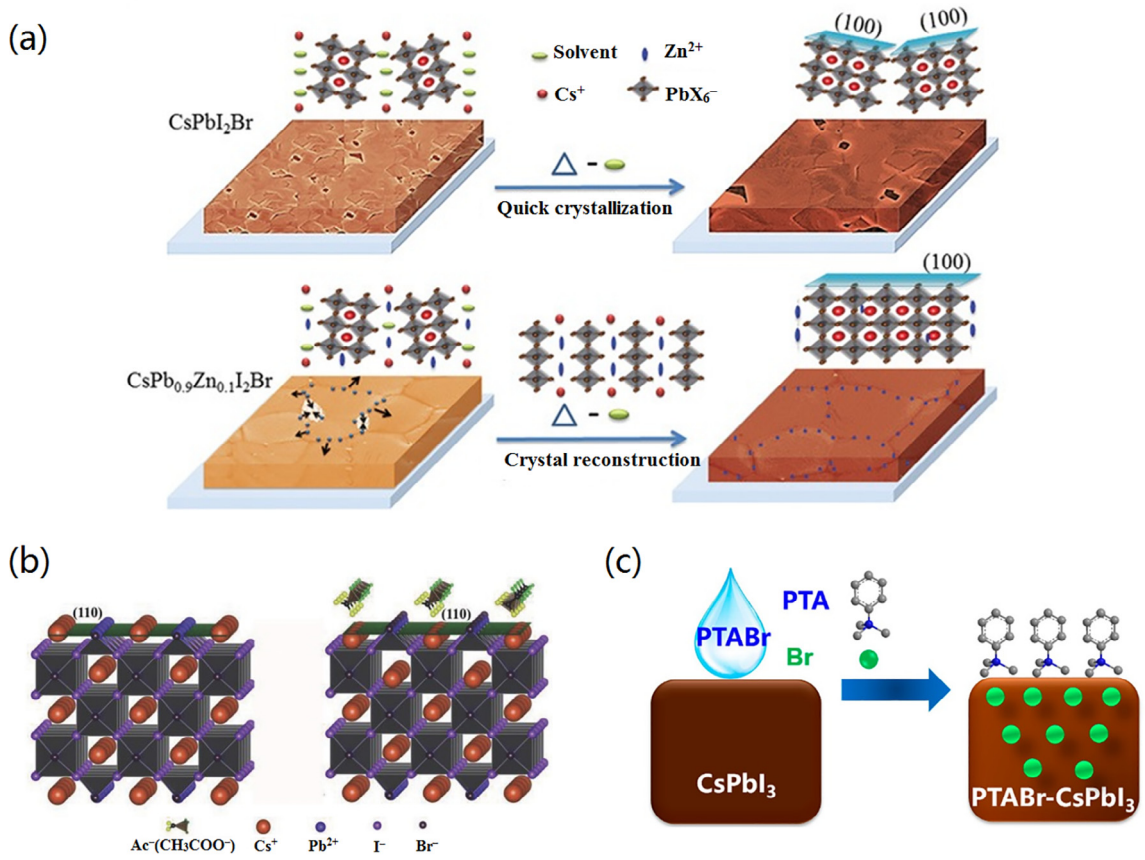

Fig. 5. (a) Nucleation and crystal growth for $CsPbI_2Br$ and $CsPb_{0.9}Zn_{0.1}I_2Br$. Reproduced with permission [48], Copyright 2019, Wiley-VCH. (b) Schematic for $CsPbI_2Br$ (1 1 0) surface without and with Ac^- interaction. Reproduced with permission [49], Copyright 2018, Wiley-VCH. (c) PTABr passivation on $CsPbI_3$ surface and gradient Br doping into the film. Reproduced with permission [14], Copyright 2018, American Chemical Society.

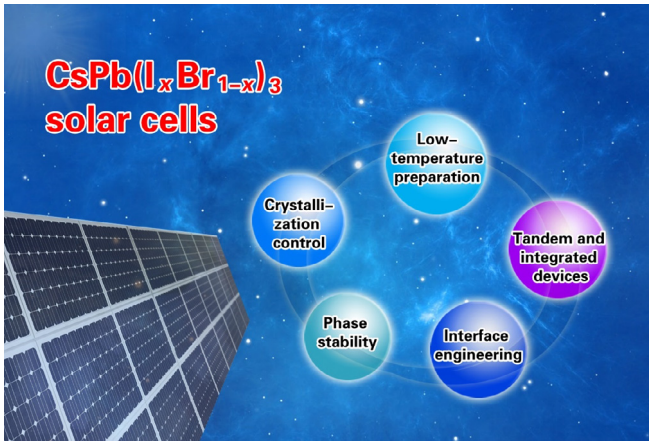

Fig. 6. Challenges and potential for $CsPb(I_xBr_{1-x})_3$ solar cells.

(4) Low-temperature preparation. Generally, high temperature is required to make high-quality $CsPb(I_xBr_{1-x})_3$ films, while this will lead to high fabrication cost and impede their applications in flexible and tandem solar cells. New approaches enabling low-temperature preparation is desired in the future.

(5) Tandem and integrated devices. $CsPb(I_xBr_{1-x})_3$ have relatively wide bandgaps (E_g of $CsPbI_3$ is 1.73 eV), and they are suitable for the front cell of perovskite/silicon tandem solar cells and for integrated device applications [56]. This is an important research direction.

Conflict of interest

The authors declare that they have no conflict of interest.

Acknowledgments

We thank the National Key Research and Development Program of China (2017YFA0206600) and the National Natural Science Foundation of China (51773045, 21572041 and 21772030) for the financial support. L. Ding thanks Miss Ding in DingXiaoShu Studio for her kind assistance in drawing Fig. 6.

Author contributions

Xue Jia prepared the manuscript. Chuantian Zuo, Shuxia Tao, Kuan Sun, Yixin Zhao, Shangfeng Yang, Ming Cheng, Mingkui Wang, Yongbo Yuan, Junliang Yang, Feng Gao, Guichuan Xing, Zhanhua Wei, Lijun Zhang, Hin-Lap Yip, Mingzhen Liu, Qing Shen, Longwei Yin, Liyuan Han, Shengzhong Liu, Lianzhou Wang, Jingshan Luo, Hairen Tan and Zhiwen Jin participated in the revision. Liming Ding directed and revised the manuscript.

References

[1] Wolf SD, Holovsky J, Moon SJ, et al. Organometallic halide perovskites: sharp optical absorption edge and its relation to photovoltaic performance. J Phys Chem Lett 2014;5:1035–9.
[2] Noh JH, Im SH, Heo JH, et al. Chemical management for colorful, efficient, and stable inorganic-organic hybrid nanostructured solar cells. Nano Lett 2013;13:1764–9.

[3] Stoumpos CC, Malliakas CD, Kanatzidis MG. Semiconducting tin and lead iodide perovskites with organic cations: phase transitions, high mobilities, and near-infrared photoluminescent properties. Inorg Chem 2013;52:9019–38.
[4] Dong Q, Fang Y, Shao Y, et al. Electron-hole diffusion lengths >175 μm in solution-grown $CH_3NH_3PbI_3$ single crystals. Science 2015;347:967–70.
[5] D'Innocenzo V, Grancini G, Alcocer MJ, et al. Excitons versus free charges in organo-lead tri-halide perovskites. Nat Commun 2014;5:3586–91.
[6] Kojima A, Teshima K, Shirai Y, et al. Organometal halide perovskites as visible-light sensitizers for photovoltaic cells. J Am Chem Soc 2009;131:6050–1.
[7] Zuo C, Ding L. Modified PEDOT layer makes a 1.52 V V_{oc} for perovskite/PCBM solar cells. Adv Energy Mater 2017;7:1601193.
[8] Zuo C, Vak D, Angmo D, et al. One-step roll-to-roll air processed high efficiency perovskite solar cells. Nano Energy 2018;46:185–92.
[9] Zuo C, Bolink HJ, Han H, et al. Advances in perovskite solar cells. Adv Sci 2016;3:1500324.
[10] Luo D, Yang W, Wang Z, et al. Enhanced photovoltage for inverted planar heterojunction perovskite solar cells. Science 2018;360:1442–6.
[11] Jiang Q, Zhao Y, Zhang X, et al. Surface passivation of perovskite film for efficient solar cells. Nat Photonics 2019;13:460–6.
[12] Wang Z, Shi Z, Li T, et al. Stability of perovskite solar cells: a prospective on the substitution of the A cation and X anion. Angew Chem Int Ed 2017;56:1190–212.
[13] Eperon GE, Paternò GM, Sutton RJ, et al. Inorganic caesium lead iodide perovskite solar cells. J Mater Chem A 2015;3:19688–95.
[14] Wang Y, Zhang T, Kan M, et al. Bifunctional stabilization of all-inorganic α-$CsPbI_3$ perovskite for 17% efficiency photovoltaics. J Am Chem Soc 2018;140:12345–8.
[15] Wells HL. Über die cäsium-und kalium-bleihalogenide. Z Anorg Chem 1893;3:195–210.
[16] Moller CK. Crystal structure and photoconductivity of cæsium plumbohalides. Nature 1958;182:1436.
[17] Marronnier A, Roma G, Boyer-Richard S, et al. Anharmonicity and disorder in the black phases of cesium lead iodide used for stable inorganic perovskite solar cells. ACS Nano 2018;12:3477–86.
[18] Sutton RJ, Filip MR, Haghighirad AA, et al. Cubic or orthorhombic? Revealing the crystal structure of metastable black-phase $CsPbI_3$ by theory and experiment. ACS Energy Lett 2018;3:1787–94.
[19] Yang Z, Surrente A, Galkowski K, et al. Impact of the halide cage on the electronic properties of fully inorganic cesium lead halide perovskites. ACS Energy Lett 2017;2:1621–7.
[20] Zeng Q, Liu L, Xiao Z, et al. A two-terminal all-inorganic perovskite/organic tandem solar cell. Sci Bull 2019;64:885–7.
[21] Swarnkar A, Marshall AR, Sanehira EM, et al. Quantum dot-induced phase stabilization of α-$CsPbI_3$ perovskite for high-efficiency photovoltaics. Science 2016;354:92–5.
[22] Jiang Y, Yuan J, Ni Y, et al. Reduced-dimensional α-$CsPbX_3$ perovskites for efficient and stable photovoltaics. Joule 2018;2:1356–68.
[23] Wang Q, Zheng X, Deng Y, et al. Stabilizing the α-phase of $CsPbI_3$ perovskite by sulfobetaine zwitterions in one-step spin-coating films. Joule 2017;1:371–82.
[24] Li B, Zhang Y, Fu L, et al. Surface passivation engineering strategy to fully-inorganic cubic $CsPbI_3$ perovskites for high-performance solar cells. Nat Commun 2018;9:1076–83.
[25] Swarnkar A, Mir WJ, Nag A. Can B-site doping or alloying improve thermal- and phase-stability of all-inorganic $CsPbX_3$ (X = Cl, Br, I) perovskites? ACS Energy Lett 2018;3:286–9.
[26] Liu F, Ding C, Zhang Y, et al. GeI_2 additive for high optoelectronic quality $CsPbI_3$ quantum dots and their application in photovoltaic devices. Chem Mater 2019;31:798–807.
[27] Liao J-F, Rao H-S, Chen B-X, et al. Dimension engineering on cesium lead iodide for efficient and stable perovskite solar cells. J Mater Chem A 2017;5:2066–72.
[28] Wang K, Jin Z, Liang L, et al. All-inorganic cesium lead iodide perovskite solar cells with stabilized efficiency beyond 15%. Nat Commun 2018;9:4544–51.
[29] Li F, Pei Y, Xiao F, et al. Tailored dimensionality to regulate the phase stability of inorganic cesium lead iodide perovskites. Nanoscale 2018;10:6318–22.
[30] Ding X, Chen H, Wu Y, et al. Triple cation additive $NH_3^+C_2H_4NH_2^+C_2H_4NH_3^+$-induced phase-stable inorganic α-$CsPbI_3$ perovskite films for use in solar cells. J Mater Chem A 2018;6:18258–66.
[31] Zhang T, Dar MI, Li G, et al. Bication lead iodide 2D perovskite component to stabilize inorganic α-$CsPbI_3$ perovskite phase for high-efficiency solar cells. Sci Adv 2017;3:e1700841.
[32] Hu Y, Bai F, Liu X, et al. Bismuth incorporation stabilized α-$CsPbI_3$ for fully inorganic perovskite solar cells. ACS Energy Lett 2017;2:2219–27.
[33] Lau CFJ, Zhang M, Deng X, et al. Strontium-doped low-temperature-processed $CsPbI_2Br$ perovskite solar cells. ACS Energy Lett 2017;2:2319–25.
[34] Bai D, Zhang J, Jin Z, et al. Interstitial Mn^{2+}-driven high-aspect-ratio grain growth for low-trap-density microcrystalline films for record efficiency $CsPbI_2Br$ solar cells. ACS Energy Lett 2018;3:970–8.
[35] Liang J, Liu Z, Qiu L, et al. Enhancing optical, electronic, crystalline, and morphological properties of cesium lead halide by Mn substitution for high-stability all-inorganic perovskite solar cells with carbon electrodes. Adv Energy Mater 2018;8:1800504.
[36] Yang F, Hirotani D, Kapil G, et al. All-inorganic $CsPb_{1-x}Ge_xI_2Br$ perovskite with enhanced phase stability and photovoltaic performance. Angew Chem Int Ed 2018;57:12745–9.
[37] Lau CFJ, Deng X, Zheng J, et al. Enhanced performance via partial lead replacement with calcium for a $CsPbI_3$ perovskite solar cell exceeding 13% power conversion efficiency. J Mater Chem A 2018;6:5580–6.
[38] Xiang W, Wang Z, Kubicki DJ, et al. Europium-doped $CsPbI_2Br$ for stable and highly efficient inorganic perovskite solar cells. Joule 2018;3:205–14.
[39] Zhang L, Li B, Yuan J, et al. High-voltage-efficiency inorganic perovskite solar cells in a wide solution-processing window. J Phys Chem Lett 2018;9:3646–53.
[40] Wang P, Zhang X, Zhou Y, et al. Solvent-controlled growth of inorganic perovskite films in dry environment for efficient and stable solar cells. Nat Commun 2018;9:2225–31.
[41] Chen W, Chen H, Xu G, et al. Precise control of crystal growth for highly efficient $CsPbI_2Br$ perovskite solar cells. Joule 2019;3:191–204.
[42] Rao H, Ye S, Gu F, et al. Morphology controlling of all-inorganic perovskite at low temperature for efficient rigid and flexible solar cells. Adv Energy Mater 2018;8:1800758.
[43] Chen CY, Lin HY, Chiang KM, et al. All-vacuum-deposited stoichiometrically balanced inorganic cesium lead halide perovskite solar cells with stabilized efficiency exceeding 11%. Adv Mater 2017;29:1605290.
[44] Bai D, Bian H, Jin Z, et al. Temperature-assisted crystallization for inorganic $CsPbI_2Br$ perovskite solar cells to attain high stabilized efficiency 14.81%. Nano Energy 2018;52:408–15.
[45] Wang Y, Zhang T, Xu F, et al. A facile low temperature fabrication of high performance $CsPbI_2Br$ all-inorganic perovskite solar cells. Solar RRL 2018;2:1700180.
[46] Jiang H, Feng J, Zhao H, et al. Low temperature fabrication for high performance flexible $CsPbI_2Br$ perovskite solar cells. Adv Sci 2018;5:1801117.
[47] Zai H, Zhang D, Liang L, et al. Low-temperature-processed inorganic perovskite solar cells via solvent engineering with enhanced mass transport. J Mater Chem A 2018;6:23602–9.
[48] Sun H, Zhang J, Gan X, et al. Pb-reduced $CsPb_{0.9}Zn_{0.1}I_2Br$ thin films for efficient perovskite solar cells. Adv Energy Mater 2019;9:1900896.
[49] Zeng Z, Zhang J, Gan X, et al. In situ grain boundary functionalization for stable and efficient inorganic $CsPbI_2Br$ perovskite solar cells. Adv Energy Mater 2018;8:1801050.
[50] Zeng Q, Zhang X, Feng X, et al. Polymer-passivated inorganic cesium lead mixed-halide perovskites for stable and efficient solar cells with high open-circuit voltage over 1.3 V. Adv Mater 2018;30:1705393.
[51] Wang Y, Zhang T, Kan M, et al. Efficient α-$CsPbI_3$ photovoltaics with surface terminated organic cations. Joule 2018;2:2065–75.
[52] Fang Z, Liu L, Zhang Z, et al. $CsPbI_{2.25}Br_{0.75}$ solar cells with 15.9% efficiency. Sci Bull 2019;64:507–10.
[53] Jia X, Liu L, Fang Z. TBAB additive for inorganic $CsPbI_{2.4}Br_{0.6}$ perovskite solar cells with efficiency beyond 15%. J Mater Chem C 2019;7:7207–11.
[54] Chen H, Xiang S, Li W, et al. Inorganic perovskite solar cells: a rapidly growing field. Solar RRL 2018;2:1700188.
[55] Ho-Baillie A, Zhang M, Lau CFJ, et al. Untapped potentials of inorganic metal halide perovskite solar cells. Joule 2019;3:938–55.
[56] Zuo C, Ding L. Bulk heterojunctions push the photoresponse of perovskite solar cells to 970 nm. J Mater Chem A 2015;3:9063–6.

Xue Jia got her B.S. degree from Hubei University in 2015. She is now a Ph.D. student in University of Chinese Academy of Sciences under the supervision of Prof. Liming Ding. Her research focuses on perovskite solar cells and organic solar cells.

Jingshan Luo received his B.S. degree from Jilin University in 2010 and Ph.D. degree from Nanyang Technological University in 2014. After that, he went to École Polytechnique Fédérale de Lausanne (EPFL) in Switzerland for postdoctoral research in the laboratory of Prof. Michael Grätzel, where he led the solar fuel subgroup later. In 2018, he joined Nankai University as a full professor and vice director of the Institute of Photoelectronic Thin Film Devices and Technology.

Hairen Tan received Ph.D. degree with distinction (cum laude) in 2015 from the Delft University of Technology. He then joined Prof. Edward Sargent group at the University of Toronto with a Rubicon Fellowship awarded by NWO in the Netherlands. In March 2018, he joined Nanjing University as a full professor. His group research focuses on perovskite solar cells and perovskite-based multijunction photovoltaic devices.

Zhiwen Jin received B.S. degree from Lanzhou University in 2011 and Ph.D. degree from Institute of Chemistry, Chinese Academy of Sciences in 2016. He joined Lanzhou University in 2018, and he is a professor in School of Physical Science and Technology. His research interests include inorganic semiconductors, thin-film photoelectric devices and device physics, particularly inorganic perovskite solar cells.

Liming Ding got Ph.D. degree from University of Science and Technology of China. He started his research on OSCs and PLEDs in Olle Inganäs Lab in 1998. Later on, he worked with Frank Karasz and Tom Russell at PSE, UMASS Amherst. He joined Konarka as a Senior Scientist in 2008. In 2010, he joined National Center for Nanoscience and Technology as a Full Professor. His research interests include perovskite solar cells, organic solar cells and photodetectors.